Design of a High-Resolution Electrostatic Cathode Ray Tube for the Flying Spot Store

By H. G. COOPER

(Manuscript received November 22, 1960)

A high-resolution electrostatically deflected cathode ray tube is required for the flying spot store of an experimental electronic switching system. This tube is used to obtain random access, by optical means, to 2.5 × 10^6 bits of information stored on a photographic plate. High degrees of both resolution uniformity and faceplate optical quality are required to achieve large storage capacity and error-free performance.

In this paper the design criteria for optimum gun performance and minimum deflection focusing are analytically and empirically evolved. A novel result of this work is a dual shield placed between the two pairs of deflection plates, which substantially reduces beam aberrations due to the deflection fringing fields. A precision tube is described that fulfills the flying spot store design objectives and has performed reliably in a field trial at Morris, Illinois.

I. INTRODUCTION

High-resolution cathode ray tubes (CRT's) with electrostatic deflection are normally limited to relatively small deflection angles because of beam-focusing effects introduced by the deflection plates. The deflection distortion causes a loss of resolution at the edges of the screen and severely limits the usable screen diameter of high-resolution tubes.

A large-capacity, high-speed, semipermanent memory,[1,2] denoted as the *flying spot store*, has recently been developed for an experimental electronic telephone switching system.[3] One of the critical components of this memory is an electrostatically deflected CRT. The tube is used to provide random access to binary information stored in the form of transparent or opaque dots on photographic plates, as shown in Fig. 1. The electron beam is deflected to the desired address on the screen of the CRT, the luminescent spot is then focused onto an array of n informa-

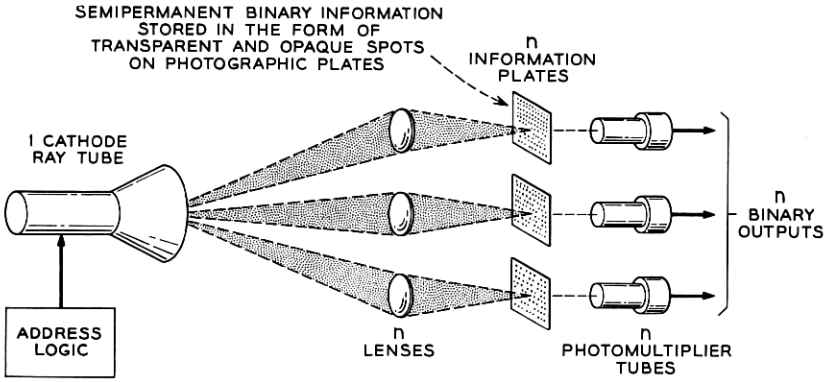

Fig. 1 — Role of the CRT in the flying spot store.

tion plates by optical lenses, and an n-digit binary output is obtained from photomultiplier tubes located behind each information plate.

System design objectives include virtually error-free performance (less than one error per 10^{10} reading operations) and a large memory capacity (2.5×10^6 bits). As a result, a precision CRT with electrostatic deflection is needed which has unusual characteristics. Among these are a small and very uniform beam size over a relatively large screen area, high deflection sensitivity, and uniform resolution over a wide beam current range without adjustment of the beam focus voltage. These points will be covered in more detail in the next section.

It was concluded that the spot size uniformity requirement at the desired resolution, screen size, etc. constituted performance appreciably better than had been previously attained. Development[4] of a CRT for the flying spot store was consequently undertaken at Bell Telephone Laboratories.

The primary objective of this article is to present the electron-optical design considerations for optimum tube performance in the system. The subjects covered, in order of presentation, are (a) tube design objectives, (b) electron gun, (c) objective lens, (d) deflection system, (e) screen, and (f) electrical characteristics of present tubes. An appreciable portion of the paper is devoted to the electrostatic deflection system, since it posed the most difficult design problem and includes a novel feature of the tube.

II. TUBE DESIGN OBJECTIVES

Development of the cathode ray tube was stimulated by system needs; thus, tube design objectives were imposed almost entirely by system

considerations. These objectives, in terms of desired tube characteristics, will be summarized in this section and serve as a basis for the three subsequent sections on tube design. Most of the values listed below have been discussed in previous articles[1,2] on system design, and others were determined in private discussions with systems personnel.

2.1 *Resolution and Spot Size Uniformity*

Cathode ray tube spot size usually refers to the diameter of the luminescent spot on the screen, which may be denoted as the *optical spot size*. This may be larger than the electron beam size (or *electrical spot size*) if there is a significant scattering of light within the screen phosphor. Experiments conducted on screen materials used in the flying spot store CRT indicated that such scattering could be made negligible if proper screen thickness and method of deposition were used. Hence it will be assumed here that electrical and optical spot sizes are the same, and the terms will be used interchangeably in the article.

A quantitative specification of spot size has long been subject to ambiguity, because of the ill-defined edge of the electron beam. Among the various methods of defining spot size are (a) shrinking raster resolution, (b) TV line resolution, and (c) the standard deviation σ of a Gaussian distribution.* The last method was chosen for this work, since experiments showed that the beam cross section in the CRT was substantially Gaussian. Another specification of spot size[1,2] is the size of a square that, when centered on the luminescent spot, will contain 90 per cent of the radiant light flux. For a Gaussian spot, the side of such a square is 4σ.

Flying spot store objectives of large storage capacity and essentially error-free operation result in CRT resolution values of $\sigma = 0.0045 \pm 0.00075$ inch. This corresponds to a spot size uniformity ratio ($\sigma_{max}/\sigma_{min}$) of $\leqq 1.4$. It should be emphasized that the tolerances on spot size must be maintained at all points on the quality screen area (6 inches square), and over the required beam-current range without changing focus potentials. The best spot size uniformity that could be obtained in commercially-developed electrostatic CRT's was a $\sigma_{max}/\sigma_{min}$ value of three, when the median σ was 0.0045 inch and the beam current was held constant at 10 microamperes.

2.2 *Accelerating Voltage*

Final CRT accelerating potential is determined by system needs for high deflection sensitivity and a high level of radiant flux from the

* See, for example, Klemperer.[5] It may be noted that σ of a Gaussian is approximately equal to one TV line or one-half a shrinking raster line.

screen. Since an improvement in one parameter is achieved only at a sacrifice in the other, a compromise must be made. On this basis, the design value for accelerating voltage was chosen as 10 kilovolts.[1,2]

2.3 *Beam Current*

Another CRT characteristic determined by the minimum permissible radiant flux from the screen is beam current. In addition, system design requires that the radiant flux must have a constant absolute value which is independent of tube life or beam location on the screen. Accordingly, variations in luminescent intensity, due to nonuniformities in screen deposition or to degradation in luminescent efficiency of the phosphor by electron bombardment, are compensated by an appropriate electronic adjustment of the beam current. Thus, an extended operating range in beam current must be provided over which the spot size limits, specified in Section 2.1, are to be maintained under conditions of constant focus voltage. It should be noted that space charge and lens aberrations produce beam size enlargements at increased beam currents.

In view of the above considerations, the required beam current operating range was selected as 4 to 20 microamperes. The value of four would be used for the most intense spot on the screen of a new tube and 20 at the dimmest location when the tube reaches end of life.

2.4 *Deflection System*

The random access feature of the flying spot store necessitates an electrostatic deflection system. In principle, magnetic coils could be used, but the power required in the deflection circuitry would be prohibitive. Objectives for the deflection system are low capacitance, less than 25 micromicrofarads per plate when driven push-pull, and an average sensitivity of 150 $\pm$ 10 volts per inch for both pairs of plates. In addition, the two sets of plates should be orthogonal to within ± 0.5 degree. Variations in deflection factor due to barrel and/or pin-cushion distortion must be less than ± 0.7 per cent over the quality screen area, which is defined later in Section 2.5.1. It is permissible to obtain the 150 $\pm$ 10 volts per inch average deflection factor by varying the final acceleration potential in the range between 9 and 11 kilovolts.

Beam focusing effects introduced by the deflection system are very deleterious to the spot size uniformity ratio. Dynamic correction for deflection focusing is frequently made by feeding part of the deflection signal back to the focus electrode(s) via an appropriate shaping circuit. This might be tolerated in the system design but is quite undesirable.

2.5 *Screen and Faceplate*

2.5.1 *Quality Screen Area*

The area of the phosphor over which tolerances on beam size, deflection factor, etc. are to be maintained is denoted the *quality screen area.* The minimum quality area is determined by many interacting system considerations, and has been specified as a square 6 inches on a side centered on the mechanical center of the faceplate.

2.5.2 *Phosphor*

The phosphor must have a short persistence ($\approx 10^{-7}$ second) to permit high-speed system operation and should possess a luminescent efficiency as high as possible. From a study of high-speed phosphors,[1,2] it was concluded that P16 was the optimum screen material. It has a decay time the order of 100 millimicroseconds and an energy efficiency of about one per cent after preaging.

Another important screen parameter is uniformity of light output from the quality area. The desired objective is less than +20 and −40 per cent variation from the median radiant flux value, in order to keep the system error rate sufficiently low.

2.5.3 *Faceplate*

The flying spot store includes a very precise optical system, which focuses the luminescent spot on the photographic information plates. Since the CRT faceplate is in the light path between the phosphor and lenses, it is a part of the optical system. One system objective is that CRT's should be interchangeable without the necessity of rewriting the information stored on their photographic plates. As a result, the faceplate is made flat (rather than curved) and must meet very rigid specifications with regard to optical flatness, thickness, plate curvature, and freedom from flaws. Briefly stated, the surface must be ground flat to within six fringes of 5890 angstroms light per inch, the thickness must be uniform (0.465 ± 0.010 inch), the radius of curvature must be greater than 1900 inches (corresponding to a bow on the axis of ±0.00375 inch measured from a plane passing through a 7.6-inch diameter circled centered thereon), and the flaw size must be maintained below 0.004-inch diameter with a minimum spacing of 0.050 inch between such flaws.

The tube design objectives discussed above are summarized in Table I.

TABLE I —SYSTEM OBJECTIVES FOR THE FLYING SPOT STORE CRT

Spot size	$\sigma = 0.0045 \pm 0.00075$ inch (for all beam currents between 4 and 20 microamperes and no change in focus potentials).
Accelerating voltage	10 kilovolts
Beam current	Variable between 4 and 20 microamperes
Deflection system	Electrostatic
Deflection factor	150 ± 10 volts per inch*
Deflection linearity	± 0.7 per cent†
Deflection plate orthogonality	90 ± 0.5 degrees
Quality area	6×6 inches square
Phosphor type	P16
Phosphor light output uniformity in the quality area	+20 and −40 per cent from the mean value
Faceplate tolerances in quality area	Flat to <6 fringes/inch of 5890 angstroms; thickness 0.465 ± 0.010 inch; minimum radius of curvature 1900 inches; maximum flaw size of 0.004 inch; flaw spacing less than 0.050 inch

* The accelerating voltage can be varied between 9 and 11 kilovolts to achieve the 150 volts per inch average deflection factor.

† Deflection factor is constant in the quality area to within ±0.7 per cent.

III. ELECTRON GUN DESIGN

Three primary objectives in the electron gun design are:

(a) small beam size at the crossover,

(b) moderate control grid transconductance, and

(c) long cathode life.

Two important factors contributing to long life are low cathode current density (or loading) and high current efficiency (the ratio of beam to cathode currents). The latter minimizes positive ion production, which in turn reduces cathode degradation due to ion bombardment. Since the ratio of surface area within the CRT to the cathode-emitting area is exceedingly large ($>10^8$), minimization of ion bombardment warrants serious consideration in the gun design.

An immersion-lens triode gun, shown in Fig. 2(a), is used in most CRT's made today. It contains three elements which focus the electrons to a small crossover located in the control grid-anode region. The crossover in turn is imaged on the screen by the objective lens. Moss[6] has investigated the triode gun in great detail. Calculations of crossover size, cathode loading, and current efficiency were carried out, using the results of Moss, for a number of triode configurations with the anode at 10 kilovolts. This approach appeared unsatisfactory because the beam current was either very low (less than 10 microamperes) or cathode loading was high (>1 ampere per cm^2), to achieve a suitably small crossover size.

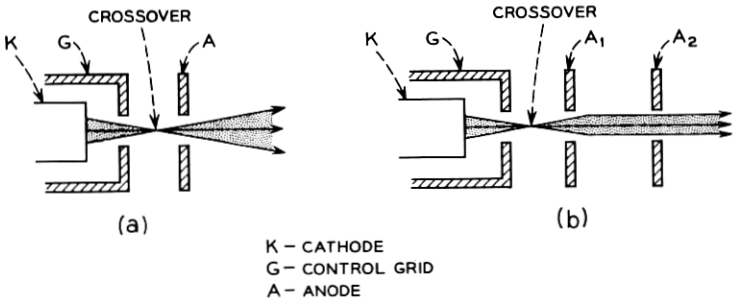

Fig. 2 — Schematics of (a) triode and (b) tetrode guns.

Much better results, which will be discussed in detail later, were obtained with the tetrode gun arrangement of Fig. 2(b), containing cathode K, control grid G, first anode A_1, and second anode A_2. Consequently, the tetrode gun was selected for the flying spot store CRT and was designed to meet the objectives outlined in Section II. The first three electrodes (K, G, and A_1) constitute an immersion-lens triode, forming a crossover in the G–A_1 space as drawn in Fig. 2(b). Therefore, the extensive knowledge available on triode guns may be applied to the tetrode front end design. A model previously developed* at Bell Telephone Laboratories for high resolution storage tubes (designed for an A_1 potential $\simeq$1 kilovolt) was selected for this purpose. It has a small crossover size and moderately high transconductance ($\approx$2 micromhos).

A very important factor affecting beam size at the screen is the electrode geometry of anodes A_1 and A_2 of the tetrode gun, where A_2 is operated at the nominal final accelerating potential of 10 kilovolts. The analysis utilized to attain a suitable design is described in the next section.

3.1 *Design of A_1 and A_2 Electrodes*

The electrode arrangement at the A_1–A_2 gap, the region in which the beam is accelerated from 1 to 10 kilovolts, interacts critically with the over-all crossover magnification M (defined as the ratio of spot size at the screen divided by the crossover size). Since the A_1–A_2 lens is converging, it should be made as weak as possible in order to minimize M. Because of its convergent action, the A_1–A_2 lens geometry also strongly affects the cathode loading and current efficiency (the fraction of cathode current that passes through the limiting aperture of the objective

* This work was done by R. W. Sears and W. E. Kirkpatrick.

lens). The latter point is illustrated by beam trajectories in Fig. 2(b), where the beam is confined closer to the axis (after it passes through the anode) for the case of the tetrode than for that of the triode. The current efficiency increases as the A_1–A_2 lens becomes more convergent (which reduces cathode loading) and also when the A_1–A_2 gap is placed closer to the crossover.

Three different A_1–A_2 configurations, shown in Fig. 3, are analyzed for crossover magnification in Appendix A. The lens constants, namely focal lengths and locations of principal planes, used in this analysis were obtained from the work of Spangenberg and Field.[7,8,9] The D_1, D_2, and S values listed in the figure were selected (from those tabulated in Ref. 7) to provide the weakest lens. The results are summarized in Fig. 4, where the magnification, M, due to all lenses between the crossover and screen is plotted as a function of the distance X between the crossover and midplane of the A_1–A_2 gap. The midplane for each geometry is indicated in Fig. 3, and the electron-optical diagram of the CRT is shown in Fig. 20(b). It may be noted from Fig. 4 that M is smallest for the A_1–A_2 configuration in (b) and that M increases monotonically with X. Thus X should be small, which, fortunately, is also the condition for maximum current efficiency. The final tetrode design incorporating a "(b)" A_1–A_2 arrangement (with a slightly reduced D_2/D_1 ratio) is included as Fig. 5. Because of electrostatic field and mechanical considerations, the distance X from the crossover to A_1–A_2 midplane could not be reduced completely to zero. One reason for this is that the crossover moves closer to the cathode as the A_1–A_2 spacing approaches zero. A 0.8-inch X value was selected, therefore, as a good compromise. Also the D_2/D_1 ratio was made small, 0.33, in order to make the A_1–A_2 lens as weak as possible. This ratio was not plotted in Fig. 4, since the lowest D_2/D_1 ratio studied by Spangenberg and Field[8] for the "(b)" geometry was 0.67.

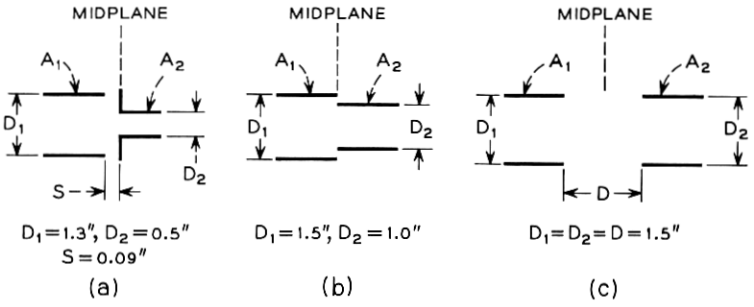

Fig. 3 — Three proposed A_1–A_2 configurations; D and S values have been selected to provide a weak A_1–A_2 lens.

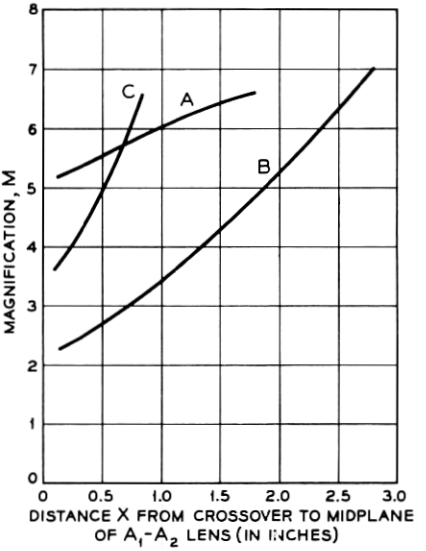

Fig. 4 — Magnification M vs. A_1-A_2 midplane position X (M = ratio of beam size at screen to crossover size). Note: M is negative for configuration (c) of Fig. 3 and positive for (a) and (b).

An important advantage of this gun design is that the average cathode loading is $\leqq 150$ milliamperes per cm^2. Also, the current efficiency is very high; for example, only about 15 microamperes of cathode current I_K are required to provide 10 microamperes of beam current I_B (67 per cent current efficiency).

Another gun feature, utilized in the flying spot store, is the capability of varying the average beam size, σ_{avg}, over a wide range by controlling

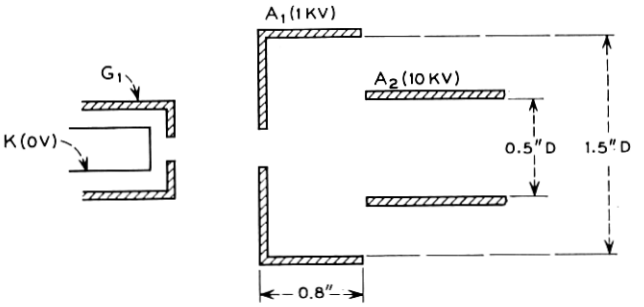

Fig. 5 — Tetrode gun design for CRT.

the voltage of A_1. This and the electrical characteristics of the tetrode gun will be presented in detail in Section VII.

IV. OBJECTIVE LENS

The crossover formed by the electron gun is imaged on the screen by the combined convergent focusing action of the A_1–A_2 lens and the objective lens [see Fig. 20(a)]. The objective lens, located close to the beam entrance side of the deflection system, provides most of the beam focusing. It also contains the limiting aperture that defines the maximum beam diameter as it passes through the objective lens and deflection system.

An electrostatic, rather than magnetic, lens was chosen for the objective for reasons of compactness and reduction of pattern distortion on the screen due to magnetic fringe fields. Fig. 6 shows the lens used, denoted *crossed-elliptical*, which has low spherical aberrations and provides orthogonal focus control. It is a four-element modified einzel (or unipotential) design, in which the first and last electrodes are both at A_2 (10 kilovolt) potential. This lens will be described in detail elsewhere[10] and only the general features will be pointed out here. (The CRT lens is a 1.5:1 scale-up of the lens described in Ref. 10.) There are two focus electrodes, A_3 and A_4, having mutually perpendicular elliptical apertures (from which the name is derived). The unique feature of the lens is substantially independent focus control in the horizontal and vertical directions by means of A_3 and A_4 respectively. It is achieved in the crossed-elliptical lens with a minimum number of electrodes. Also, the axial

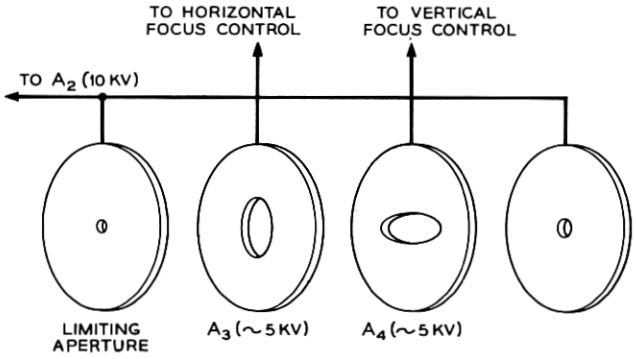

Fig. 6 — Crossed-elliptical lens.

distance occupied by the lens is very small. Both A_3 and A_4 operate at a potential near 5 kilovolts in the CRT design.

4.1 *Advantages of the Crossed-Elliptical Lens*

There are several means by which the independent focus properties of the lens are utilized in the flying spot store CRT:

i. It permits astigmatism correction at the objective lens, rather than at the deflection system. This is advantageous in the design of the deflection amplifier for the flying spot store.

ii. The conditions for optimum focus (best spot size uniformity ratio) can be attained more conveniently. The beam-positioning servo-loop of the flying spot store contains separate vertical and horizontal bar patterns located in the plane of the photographic plates. From them, it can be ascertained when best vertical and horizontal focus is reached, and the adjustment can be made quickly with virtually no interaction in the two directions.

iii. The crossed-elliptical lens can provide independent dynamic deflection focus correction; at present this is not used, but it is available if needed. Circuitry for dynamic correction with this lens has been developed in connection with the barrier-grid storage tube.[10,11]

4.2 *Lens Location and Length of CRT*

Magnification of the objective lens (M_2 in Appendix A) is determined by the spot size required at the screen, crossover size, and magnification M_1 of the A_1–A_2 lens. With the tetrode gun design described in Section 3.1, it was found that the image-to-object distance ratio q_2/C of the objective lens (see Fig. 20) should be about 5 to obtain the required average beam size, σ_{avg}, of 0.0045 inch. The image distance q_2, from the center of the objective lens to the screen, is determined almost entirely by the minimum permissible distance from the beginning of the deflection system to the screen. This in turn is defined by the amount of deflection focusing that can be tolerated. In the Section V it is concluded that q_2 should be 25 inches. Hence the object distance C from crossover to the objective lens, is equal to 5 inches. The lens is placed as close to the entrance of the deflection system as fringing field aberrations will permit. In the CRT, this axial spacing (1.0 inch) was made twice the entrance separation (0.5 inch) of the gun's set of deflection plates.

The over-all tube length is equal to the cathode-to-screen distance ($C + q_2$) plus the axial length needed at the cathode end for leads,

supports, stem, and base (about 5 inches for this CRT). Hence the total tube length becomes $(C + q_2 + 5)$, which is approximately 35 inches.

4.3 *Limiting Aperture*

The electron beam diameter, as it passes through the objective lens and deflection system, is an important tube-design parameter. It is one of the dominant factors that determine lens and deflection aberrations. Thus it influences both the average spot size σ_{avg} and the uniformity ratio $\sigma_{max}/\sigma_{min}$.

A very suitable position for the limiting aperture was found to be at the first electrode of the crossed-elliptical lens (see Fig. 6). Effects of secondary emission from that location were negligible, and it was also convenient from mechanical considerations. Two aperture diameters were studied, 0.113 and 0.075 inch. The spot size uniformity ratio was slightly better (5 to 10 per cent) for the smaller aperture, but cathode loading was increased considerably. Since spot size objectives could be met with the 0.113-inch aperture, it was used in the final design.

V. DEFLECTION SYSTEM

The most formidable CRT design problem, and the area where the greatest improvement over previously existing tubes was needed, was that of the electrostatic deflection system. The primary problem was reduction of deflection focusing and aberration effects to the point where sufficient uniformity in beam size would be achieved over the relatively large quality screen area.

The general approach was as follows. First, the deflection plates were contoured to maximize sensitivity. The distance from the screen to the point where the beam enters the deflection system was then selected to maintain deflection focusing effects appropriately small. Finally, the separation, length, and termination for the two pairs of plates were designed for the lowest $\sigma_{max}/\sigma_{min}$ ratio. Clearly, the optimum spot uniformity is achieved when the maximum spot enlargement produced by the vertical plates is equal to that of the horizontal set. The problem then is to evaluate quantitatively, the spot size enlargement for a given electrostatic deflection system, which will be done below.

5.1 *Plate Contour*

It has long been known[12] that the sensitivity of electrostatic deflections can be optimized by shaping them to the beam contour at the maximum

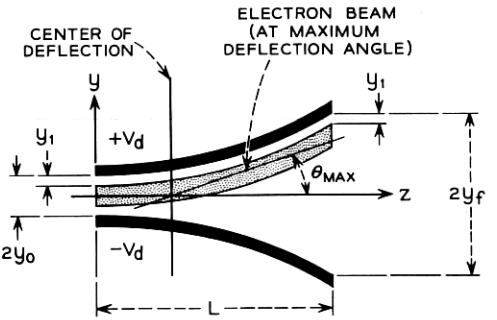

Fig. 7 — Deflection plate contour for maximum sensitivity: V_d is measured relative to average deflection plate potential, V_0 ; distance y_1 from beam edge to deflection plate is constant for all values of z.

deflection angle. Under these conditions, as may be seen from Fig. 7, the beam edge is always a constant distance y_1 (perpendicular to the axis) from the positive plate. The equation[12] for the optimum shape, where the axial dimension z is expressed as a function of the transverse distance y, may be written as

$$z - z_0 = 2y_0 \left(\frac{V_0}{V_d}\right)^{\frac{1}{2}} \int_0^{\sqrt{\ln (y/y_0)}} e^{u^2}\, du. \tag{1}$$

Parameters in (1), illustrated in Fig. 7, are the initial plate separation $2y_0$, the accelerating (or average deflection plate) potential V_0 , and the maximum push-pull deflection voltage V_d (measured relative to V_0). It may be noted that the so-called "peak-to-peak" deflection voltage is $4V_d$, since each plate has a maximum variation of $\pm V_d$. A boundary condition is that $z = z_0$ when $y = y_0$. Equation (1) is an integral for which no closed-form solution was found. Fortunately, it is the same as that for space charge spreading in a cylindrical beam, and solutions have been tabulated in generalized graphical form (Ref. 13, p. 149). A specific plot of interest in deflection plate design is

$$\frac{y}{y_0} \quad \text{vs.} \quad \frac{z - z_0}{2y_0 \left(\frac{V_0}{V_d}\right)^{\frac{1}{2}}},$$

which is included as Fig. 8. The final plate separation, $2y_f$ in Fig. 7, is given by the value of y when z is equal to the deflection plate length L. All intermediate points can be obtained from Fig. 8 once V_0 , V_d , and y_0 are determined.

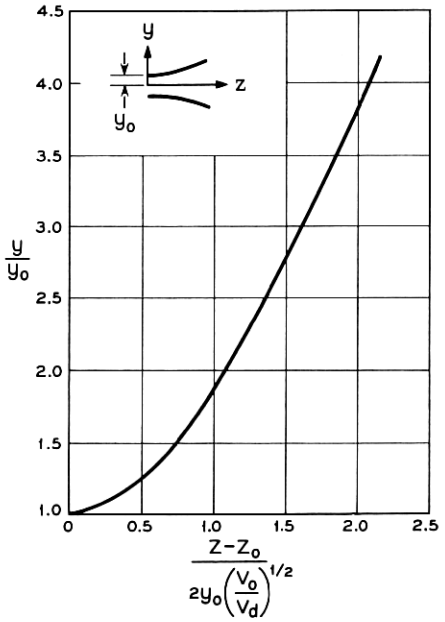

Fig. 8 — Fundamental curve for designing deflection plates contoured for maximum sensitivity.

5.2 *Spot Size Enlargement Produced by Deflection Focusing*

Fig. 9 depicts the phenomenon of deflection focusing. The trajectories of edge electrons, as the beam passes from the deflection system to the screen, are shown for zero and maximum deflection in Figs. 9(a) and 9(b) respectively. With no deflection, the electrons are converged to a point on the screen by the objective lens. Upon application of deflection voltages, the electrons are given additional convergence (in the direction of deflection only) by the deflecting field such that the edge electrons cross over before reaching the screen. This results in an enlarged spot in the direction of deflection and is denoted as *deflection focusing*. A qualitative explanation of the effect is that the electrons nearest to the positive deflection plate are at a higher average potential than other electrons in the beam. Consequently, they pass through the deflecting field faster. Since the electrostatic deflection field, E, is essentially constant in the y direction, the faster electrons are deflected less than are those moving more slowly. Hence the beam is converged by the deflection system and comes to a focus (in the y direction) in front of the screen. The electrostatic plates may then be regarded as a cylindrical

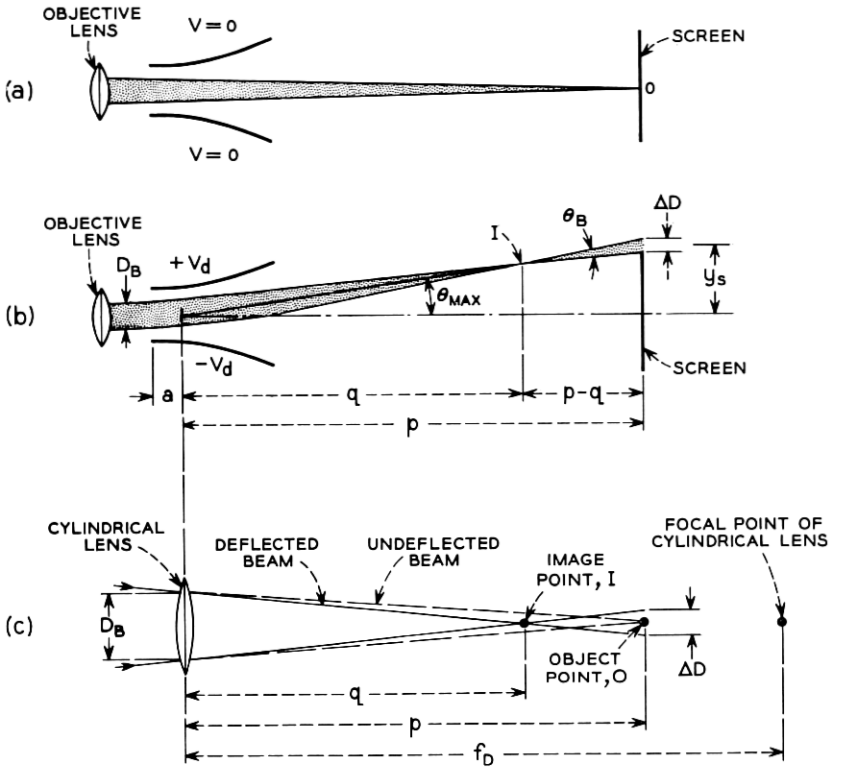

Fig. 9 — Illustration of deflection focusing for (a) undeflected beam; (b) beam at maximum deflection angle; (c) lens equivalent of deflection plates.

converging lens with an associated focal length f_D, as sketched in Fig. 9(c).

5.2.1 *Deflection Plate Focal Length, f_D, for Contoured Deflection Plates*

Pierce (Ref. 13, pp. 41–46) has derived the generalized equation for deflection plate focal length f_D, which is

$$\frac{1}{f_D} = 2\int_0^s \frac{1}{\cos^2\varphi}\left(\frac{d\theta}{ds}\right)^2 ds. \tag{2}$$

In (2), s is the distance along the electron path, φ is the angle between the deflection field E and the normal to the electron path, and θ is the angle between the electron path and the tube axis.

Focal length, f_D, can now be evaluated for the contoured plates which

were discussed in Section 5.1. It will be assumed that the deflection angle, θ, is sufficiently small that (a) $\cos \varphi \simeq 1$ (the deflecting field is normal to the path); (b) $s \simeq z$, where z is the axial distance; and (c) $\tan \theta \simeq \theta$. In practice, θ is usually less than 10 degrees, so that all three of the above should be good approximations (neglecting fringing fields). Equation (2) can then be written as

$$\frac{1}{f_D} = 2 \int_0^L \left(\frac{d \tan \theta}{dz} \right)^2 dz , \tag{3}$$

where L is the total axial length of the deflection plates. From the derivation[12] of (1) for the contoured plates, it can be shown that

$$\frac{d \tan \theta}{dz} = \frac{V_d}{2 V_0 y} \qquad \text{and} \qquad dz = \frac{dy}{\left(\frac{V_d}{V_0} \ln \frac{y}{y_0} \right)^{\frac{1}{2}}}, \tag{4}$$

where V_d, V_0, and y are defined in Section 5.1 and Fig. 7. From (4) and the substitution $y/y_0 = e^{u^2}$, (3) becomes

$$\frac{1}{f_D} = \frac{\sqrt{\pi}}{2 y_0} \left(\frac{V_d}{V_0} \right)^{\frac{1}{2}} \operatorname{erf} \left(\ln \frac{y_f}{y_0} \right)^{\frac{1}{2}}, \tag{5}$$

where erf is the error function* for which

$$\operatorname{erf} X \equiv \int_0^X \frac{2}{\sqrt{\pi}} e^{-u^2} \, du .$$

In Appendix B, f_D is related to the "zero spot size enlargement," ΔD, of a beam with zero undeflected beam size [see Fig. 9(c)]. From (17), ΔD is given by the equation

$$\Delta D = \frac{p}{f_D} D_B , \tag{6}$$

where p is the distance from the center of deflection to screen and D_B is the beam diameter at the deflection plates. The enlargement $\Delta\sigma$ of a Gaussian beam, unlike ΔD, is a function of beam size σ for any given deflection plate design. Hence the zero spot size enlargement, ΔD, is a fundamental parameter of a deflection system, where $\Delta\sigma$ may be obtained from the curve of Fig. 22 for any specific σ and ΔD.

5.3 *Deflection System to Screen Distance, Plate Separation, and Plate Length*

For a fixed distance, $z_{D\text{-}S}$, from the deflection system to screen, two critical parameters in the design of a precision electrostatic deflection

* See, for example, Peirce.[14]

system are the plate separation $2y_0$ and the axial plate length L. A small separation increases deflection sensitivity, but at the same time it enhances beam aberrations produced by fringing fields. Similarly increasing the plate length diminishes the deflection focusing effects (Ref. 13, pp. 41–46), but increases tube length and plate capacitance. Hence not all of the tube characteristics can be optimized simultaneously, and compromises must be made in accordance with design objectives.

The deflection plate design procedure used for the CRT can be summarized in two basic steps:

1. The plate length, L, was computed for both pairs such that the maximum spot enlargement, $\Delta\sigma$, due to deflection focusing was just equal to the maximum permissible value. This allows the deflection plate-to-screen distance $z_{D\text{-}S}$ to be minimized.

2. After L was obtained, the spacing $2y_0$ was made as large as deflection sensitivity requirements would permit. This minimized fringing field aberrations.

As discussed previously, the spot size objective was $\sigma = 0.0045 \pm 0.00075$ inch. The ΔD and $\Delta\sigma$ values computed in Appendix B are based on best focus at the screen center. Although this restriction permits a formulation of deflection design theory, it does not yield the best spot uniformity. That is, the CRT focus control should be adjusted for minimum beam diameter at a screen location intermediate between the center and corner to achieve best performance. Experience indicates that a midway point is about optimum and that, under this condition of best focus, the $\Delta\sigma = \sigma_{\max} - \sigma_{\min}$ value is about one half of that computed when it is assumed that the best focus is at the screen center. Hence the $\Delta\sigma$ value used to obtain ΔD from Fig. 23 was $2(\sigma_{\max} - \sigma_{\min})$. This is 0.0015 inch $\times$ 2 = 0.003 inch, which corresponds to $\Delta D = 0.021$ inch. Theoretically this ΔD figure should be used for both sets of plates, but experience indicated that the calculated ΔD should be slightly less for the target set than for the gun plates, in order that the experimentally observed $\Delta\sigma$'s would be the same for both. Thus ΔD values of 0.025 and 0.018 inch were selected for gun and target plates respectively. The result was that this overshot the goal slightly (they should have been closer together) but not enough to warrant deflection plate redesign.

It should be stressed that the primary objective of the deflection design procedure outlined below is to equalize ΔD (and hence $\Delta\sigma$) for the two pairs of plates. The particular ΔD value selected depends on the CRT to be designed but, once parameters such as deflection-to-screen distance $z_{D\text{-}S}$, accelerating voltage V_0, screen size y_s, etc. have been specified, the best $\sigma_{\max}/\sigma_{\min}$ ratio will be achieved *when the observed* ΔD *(or* $\Delta\sigma$*) is made the same for both horizontal and vertical deflection plates.*

The design values for spacings $2y_0$ and $2y_f$, deflection-to-screen distance $z_{D\text{-}S}$, plate length L, and zero beam size enlargement ΔD were obtained by the following iterative procedure:

1. A value is assumed for distance $z_{D\text{-}S}$ from the beginning of the deflection system to the screen and also for the initial plate separation $2y_0$. The location of center of deflection is estimated and the distance p from it to the screen is computed.

2. From the estimated values of p and the required screen deflection distance y_s, the approximate deflection angle θ (taken relative to the axis) is computed, where $\tan \theta = y_s/p$.

3. The deflection plate flare ratio y_f/y_0 is computed from the equation

$$\frac{y_f}{y_0} = e^{V_0/V_d \tan^2 \theta}$$

[obtained by integrating (4)], where $V_0 = 10$ kilovolts and $V_d = 250$ volts are fixed by tube design objectives. From this ratio and the assumed $2y_0$ value, the final plate separation $2y_f$ is obtained.

4. From the computed y_f/y_0 ratio, the quantity

$$\frac{z_f - z_0}{2y_0 \sqrt{\frac{V_0}{V_d}}}$$

is obtained from Fig. 8, and the axial plate length L, which is equal to $z_f - z_0$, is determined (y_0, V_0, and V_d are known).

5. The exact location of center of deflection (quantity a in Fig. 9) is calculated from the equation

$$a = L - \left(\frac{y_f - y_0}{\tan \theta}\right).$$

If it differs from the value assumed in step 1, steps 2 to 5 are repeated with the new a value. The zero spot size enlargement ΔD is determined using (5) and (6), where $\Delta D = pD_B/f_D$.

If the ΔD value obtained in step 5 differs appreciably from that desired, as it almost certainly will after the first attempt, then the values assumed for $z_{D\text{-}S}$ and/or $2y_0$ are altered until the proper ΔD is attained. This iterative procedure is followed first for the pair of plates nearest the electron gun (gun set) and then for the target set until the desired ΔD values are reached for the two pairs of plates. After some experience, the final design can be reached after about six series of computations. Table II includes the final sequence of calculations for the CRT design. Important design values are: (a) distance from the gun plates to the

TABLE II—FINAL VALUES FOR DEFLECTION PLATE DESIGN

Fixed parameters.....	V_0 = 10 kilovolts; V_d = 250 volts;* y_s = 3 inches; $D_{\text{lim.ap.}}$ = 0.113-inch diameter	
Assumed parameters....	$2y_0$ = 0.500 inch, $z_{D\text{-}S}$ = 24.5 inches; axial distance between the two pairs of deflection plates = 0.75 inch	
	Gun Set	Target Set
$\tan\theta \left(= \frac{y_s}{p}\right)$	$\frac{3 \text{ inches}}{23.0 \text{ inches}} = 0.130$	$\frac{3 \text{ inches}}{18.35 \text{ inches}} = 0.165$
θ (relative to axis)	7.5 deg	9.4 degrees
$\frac{y_f}{y_0} = e^{V_0/V_d \tan^2\theta}$	1.98	2.98
$\frac{L}{2y_0}\left(\frac{V_0}{V_d}\right)^{\frac{1}{4}}$ (from Fig. 8)	1.07	1.60
Center of deflection, $\left(a = L - \frac{y_f - y_0}{\tan\theta}\right)$	1.5 inches	2.0 inches
Center of deflection to screen, p	23.0 inches	18.35 inches
$D_B = \frac{D_{\text{lim.ap.}}p}{z_{D-S} + 1 \text{ inch}}$†	$\frac{0.113 \text{ inch} \times 23.0 \text{ inches}}{25.5 \text{ inches}} = 0.102 \text{ inch}$	$\frac{0.113 \text{ inch} \times 18.35 \text{ inches}}{25.5 \text{ inches}} = 0.081 \text{ inch}$
$\frac{1}{f_D} = \frac{\sqrt{\pi}}{2y_0}\left(\frac{V_d}{V_0}\right)^{\frac{3}{4}} \cdot \text{erf}\left(\ln\sqrt{\frac{y_f}{y_0}}\right)$	$\frac{1}{95 \text{ inches}}$	$\frac{1}{83 \text{ inches}}$
$\Delta D = \frac{D_B p}{f_D}$	0.025 inch	0.018 inch

* Corresponding to a deflection sensitivity of approximately 150 volts per inch.
† Distance from objective lens to entrance of the gun plates is 1 inch.

screen $z_{D\text{-}S}$ = 24.5 inches, (b) initial plate separation $2y_0$ = 0.500 inch for both sets of plates, and (c) axial lengths of 3.4 inches and 5.1 inches for gun and target plates respectively. It may be noted that, with a limiting aperture of 0.113-inch diameter at the objective lens, the electron beam occupies only about 20 to 25 per cent of the initial plate spacing $2y_0$. Considerably higher deflection sensitivity (lower V_d values) could be achieved by decreasing $2y_0$, but this was not done since the sensitivity was adequate for system design. Also, fringing field and deflection focusing aberrations would then be increased. The plate contour (y versus z) can be obtained from Fig. 8, letting $z = L$ when $y = y_f$.

5.4 *Effects of Fringing Fields*

In all of the deflection-system considerations thus far, fringing fields have been neglected. During the course of the CRT development, it was found that very appreciable aberrations were introduced by fields between the two sets of conventionally designed electrostatic plates. For purposes of discussion, the gun and target sets of plates will be denoted as the vertical and horizontal pairs respectively. Similarly, the respective enlargements along the vertical and horizontal axes are designated $\Delta\sigma_V$ and $\Delta\sigma_H$. The effects of deflection aberrations, as observed on the screen, are shown in the distortion patterns of Fig. 10, where enlargements are exaggerated for purposes of illustration. The left side of the figure depicts the spot distortion pattern expected from theory, where the deflection plates are assumed to be converging cylindrical lenses that distort the beam in the direction of deflection only. It may be noted, for example, that when only vertical deflection voltages are applied the beam is expected to enlarge only along the vertical axis (the enlargement being denoted as $\Delta\sigma_{V_0}$). When measurements were made on experimental tubes, however, the distortion pattern observed was as shown at the right of Fig. 10. It differs considerably from the expected, or "normal," pattern and consequently is denoted as "abnormal." The normal spot size enlargements are denoted as $\Delta\sigma_{V_0}$ and $\Delta\sigma_{H_0}$, and the abnormal ones as $\Delta\sigma_{V_1}$ and $\Delta\sigma_{H_1}$. As will be described below, the abnormal focusing effects are due to the fringing fields between the two pairs of plates, and they can be restored to a normal pattern by appropriate shaping of these fields.

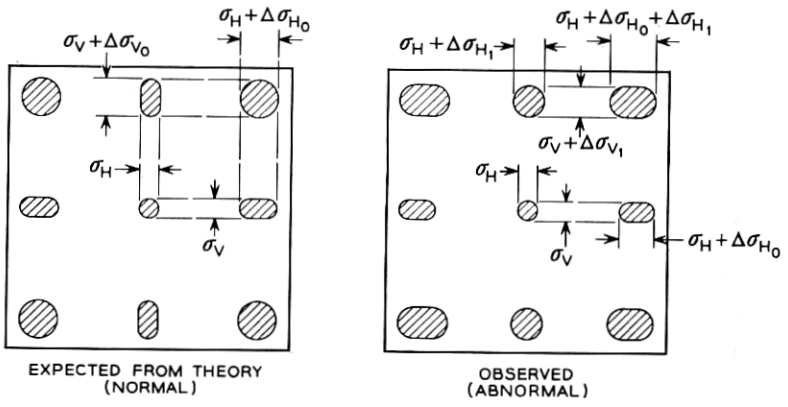

Fig. 10 — Deflection distortion patterns as observed on the CRT screen.

5.4.1 *Explanation of Distortion Pattern*

A feature of the abnormal pattern worth noting is that the beam behaves essentially normally for horizontal deflection only (where $\Delta\sigma_V \simeq 0$ and $\Delta\sigma_H \simeq \Delta\sigma_{H_0}$). When the beam was only deflected vertically, however, $\Delta\sigma_V$ was less than expected, but the beam enlarged nearly as much along the horizontal as in the vertical direction ($\Delta\sigma_{H_1} \simeq \Delta\sigma_{V_1}$). Thus, when the beam is deflected to the corners of the raster, the horizontal enlargements $\Delta\sigma_{H_0}$ and $\Delta\sigma_{H_1}$ are substantially additive. This results in a highly egg-shaped beam at the corners and the $\sigma_{\max}/\sigma_{\min}$ ratio reaches exceedingly large values. It should be noted that it is primarily the vertical deflection that produces the tremendously large horizontal enlargement at the corners. Also, the observed enlargement $\Delta\sigma_{V_1}$ in the vertical direction is less than $\Delta\sigma_{V_0}$ predicted by theory. This is not very consoling, however, since the damage to spot size uniformity already has been done.

The abnormal distortion pattern can be explained qualitatively by the focusing action of the fringing field between the two sets of deflection plates. Section A-A of Fig. 11 is a view of this interplate fringing field looking down the axis toward the screen with only vertical deflection voltages applied. There are skew-line electric forces acting on the beam, which are schematically shown in the figure. The beam position in the fringing field is above the axis, near the positive vertical plate. Looking qualitatively at the net focusing action, it may be seen (from the diagram of forces acting on peripheral electrons in Fig. 11) that the fringing field is *diverging* along the vertical and *convergent* in the horizontal direction.

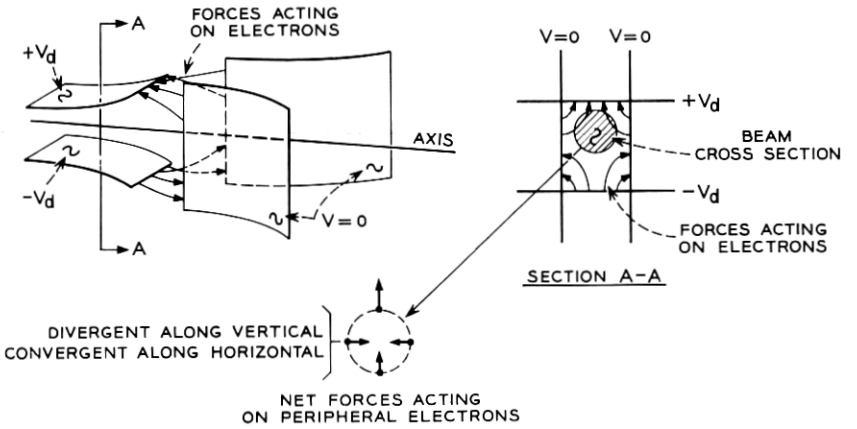

Fig. 11 — Focusing action of interplate fringing field without shields.

Hence there is a net horizontal convergence even though the beam is deflected only vertically, which explains the $\Delta\sigma_{H_1}$ of Fig. 10. Also, the net divergent action of the interplate fringing field in the vertical direction cancels out some of the predominant convergence of the vertical deflection field. Consequently, as previously noted, the amount of spot size enlargement $\Delta\sigma_{V_1}$ is less than the $\Delta\sigma_{V_0}$ calculated.

5.5 *Dual Deflection Shield*

It is clear that the abnormal deflection focusing can be produced by the skew fringing fields in the region between the two sets of plates. These skew lines are in turn caused by overlap or interpenetration of the fringing fields where the beam exits the vertical plates and enters the horizontal set. Hence some type of isolation (or shielding) of the two fields is needed. A single shield between plates, as indicated in Fig. 12(a), is frequently used, presumably to perform fringing-field isolation and provide electrostatic shielding between horizontal and vertical deflection signals. When the single shield was evaluated in experimental testers, no improvement in resolution uniformity was found. As may be seen from the data presented in Fig. 13, $\Delta\sigma_{H_1}$ increased while $\Delta\sigma_{H_0}$ decreased when just a single shield was used. This represents an enhanced abnormal effect, and the $\sigma_{\max}/\sigma_{\min}$ ratio remained very high but about constant for all the no-shield and single-shield testers that were studied.

It was concluded that more complete shielding was needed between the two pairs of plates. One approach to the problem is to increase the axial separation between the two plate pairs, but this has disadvantages of increasing tube length and/or the deflection angle of the target set of plates. An alternative method is to provide better electrostatic shielding between the two interplate fringing fields. The dual shield of Fig. 12(b)

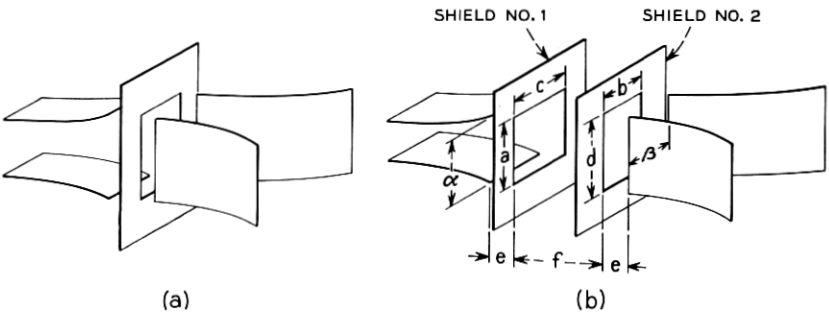

Fig. 12 — Deflection shields: (a) single; (b) dual.

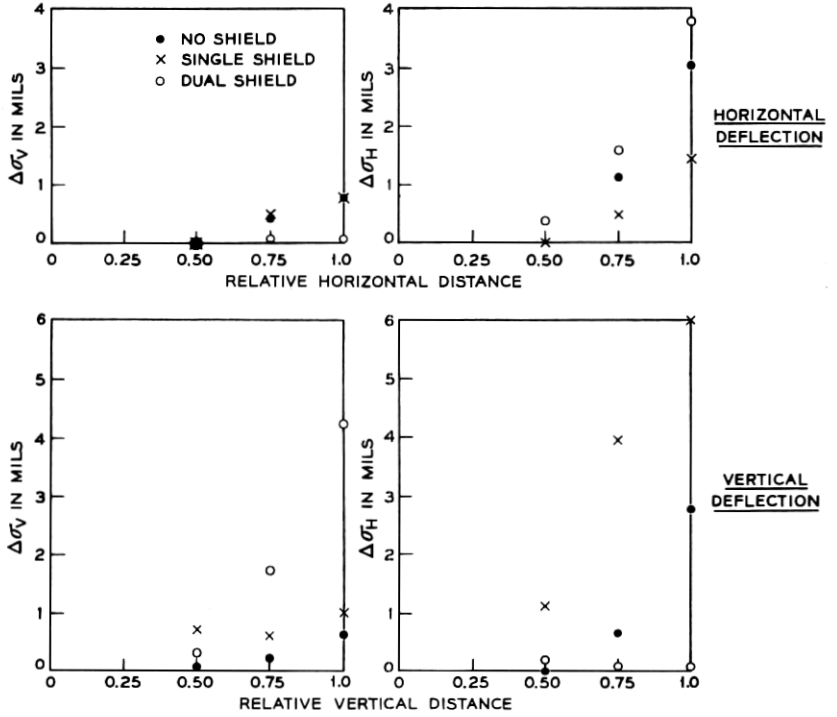

Fig. 13 — Spot distortion as a function of distance deflected on screen.

was devised for this purpose. It is compact and, as may be seen from Fig. 13, it virtually eliminates the abnormal deflection focusing effect (both $\Delta\sigma_{H_1}$ and $\Delta\sigma_{V_1}$ are very nearly normal for the dual shield). The normal spot size enlargements, $\Delta\sigma_{V_0}$ and $\Delta\sigma_{H_0}$, are increased with the dual shield. In spite of this, the over-all result is a marked improvement in resolution uniformity since the sum of $\Delta\sigma_{H_0} + \Delta\sigma_{H_1}$ is less (see Section 5.4.1).

The two shields have mutually perpendicular rectangular apertures, in which the short dimensions, a and b in Fig. 12(b), are approximately equal to the separation, α and β respectively, of the nearest set of plates. The long dimensions, c and d, are made as large as is mechanically feasible. Plate-to-shield axial spacing e is as low as possible, and the shield separation f (0.5 inch for the CRT) is just large enough to provide adequate fringing field isolation. Basically the dual shield concentrates the exit field of the vertical set of plates and the entrance field of the horizontal pair such that the field overlap is effectively zero. The shields are

operated at the average deflection plate potential (final accelerating voltage of the CRT) and therefore no external leads to the shields are necessary.

5.6 *Alignment of Beam Axis with Midplane of Target Deflection Plates*

With the high degree of precision required from the flying spot store CRT, there are many tube dimensions that must be held to unusually small tolerances. One of the most important considerations in this regard is alignment of the electron beam with the center (or midplane) of the horizontal (target) deflection plates. The degree of accuracy required was studied by applying a horizontally deflecting magnetic field between the objective lens and target set of plates. It was found that the spot size uniformity ratio was degraded noticeably when the beam was deviated only slightly from horizontal deflection plate midplane. The maximum amount of misalignment which could be tolerated in the CRT was estimated as ± 0.025 inch. This necessitates very precise alignment of the tetrode gun and objective lens axes with that of the target deflection plates. From a similar investigation at the gun plates, it was concluded that the degree of alignment with the midplane of the vertical set is not nearly so critical.

VI. FACEPLATE AND SCREEN

The screen consists of a P16 phosphor settled on a flat faceplate and then aluminized. The phosphor decay time (or persistence) is approximately 100 millimicroseconds after preaging. A component of radiated light with longer decay time is aged out by a treatment of 0.04 coulomb per cm^2 of cumulative charge at 10 kilovolts (this takes about three days with $I_B = 50$ microamperes). The aging treatment also yields a more uniform light output over the screen area during system use, which prolongs the screen life. A screen weight of 1.5 milligrams per cm^2 yielded the optimum light output for the batch of P16 material that was used. Measurements of the electron beam size and optical observations of the luminous spot size made on the same CRT showed that the increase in σ due to light scatter in the screen was less than one per cent, when σ was 0.0045 inch.

Another screen requirement was uniformity of light output (radiant flux) from the quality area. The necessary uniformity was achieved using screen fabrication techniques developed by G. Helmke and A. Pfahnl. Maximum variations in radiant flux are typically maintained between $+20$ and -30 per cent from the median flux.

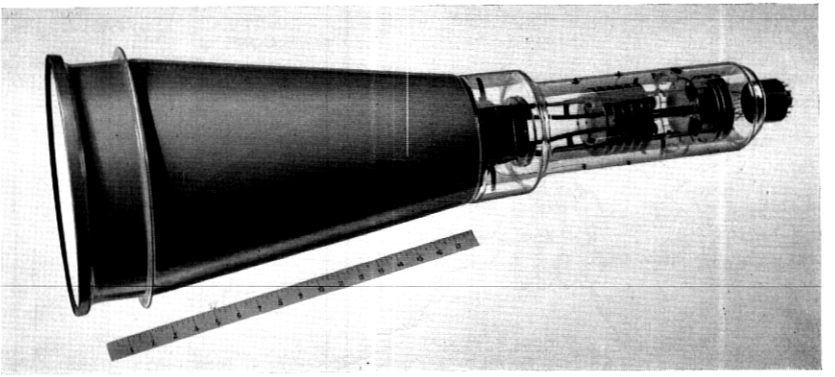

Fig. 14 — The CRT for the flying spot store.

As discussed in Section II, the glass faceplate must be of optical quality, very free from flaws and must meet rigid flatness and dimensional specifications. The objectives on glass blemishes were 0.004 inch maximum flaw diameter with a minimum spacing of 0.050 inch between flaws. This was achieved* by custom melting the glass, rolling to the proper thickness, and selecting only those areas that met specified tolerances. The plates were then cut, ground to an "F" optical quality surface, and sealed into a metal rim. The radius of faceplate curvature was maintained above 1900 inches (after tube evacuation) by means of special sealing techniques. The faceplate diameter is 10 inches, which permits an $8\frac{1}{2}$-inch diameter quality area and results in a maximum tube diameter of $10\frac{1}{2}$ inches.

VII. CHARACTERISTICS AND PERFORMANCE

A completed tube is shown in Fig. 14, with a schematic cutaway view in Fig. 15. Typical operating voltages and other tube characteristics are tabulated in Table III. Of the various characteristics listed in the table, it may be noted that the degree of spot size uniformity is somewhat better than the original system objectives. In the average tube, the spot size σ is maintained within the range 0.0045 ± 0.0006 inch for constant focus and over a beam current range between 4 and 20 microamperes. Beam current, I_B, is plotted as a function of both cathode current, I_K, and control grid bias, V_g, in Fig. 16 for $V_{A_1} = 625$ and 1000 volts and

* Faceplate development, as well as all mechanical design, was done by a group under the direction of C. Maggs and J. W. West.

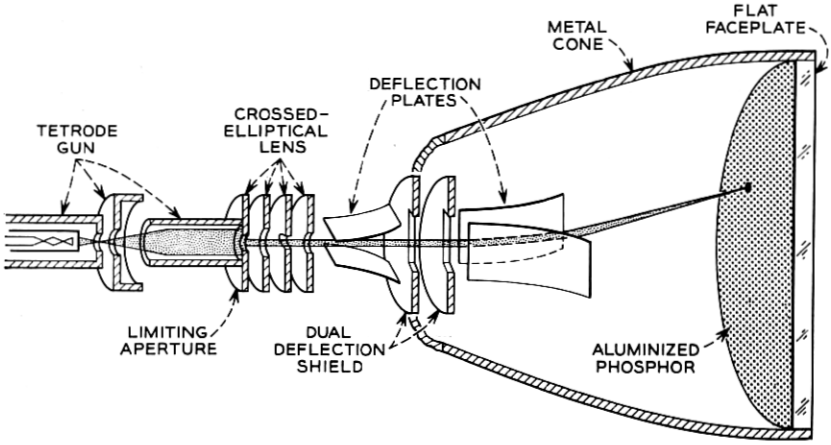

Fig. 15 — Cutaway schematic view of the flying spot store CRT.

TABLE III—FLYING SPOT STORE CRT CHARACTERISTICS

Typical Operating Potentials*	
First anode (A_1)	0.5 to 1.0 kilovolt
Second anode (A_2)	10 kilovolts
Vertical focus anode (A_4)	5 kilovolts
Horizontal focus anode (A_3)	5 kilovolts
Control grid	
(a) cutoff	−100 to −70 volts
(b) operating	−90 to −50 volts
Heater	6.8 volts
Tube Characteristics	
Deflection sensitivity	150 ± 10 volts per inch
Beam current, I_B	4 to 20 microamperes
Maximum over-all length	36 inches
Maximum over-all diameter	10½ inches
Minimum faceplate radius of curvature	1900 inches
Quality area	6 × 6 inches
Screen	
(a) phosphor type	P16 (aluminized)
(b) uniformity of radiant flux	+20 per cent, −30 per cent from average flux
Spot size σ (for I_B between 4 and 20 microamperes at constant focus)	0.0045 ± .0006 inch
Spot size uniformity ratio, $\sigma_{max}/\sigma_{min}$	<1.3
Deflection plate capacitance (per plate for push-pull deflection)	16 μμf (gun set) 24 μμf (target set)

* All expressed relative to cathode potential.

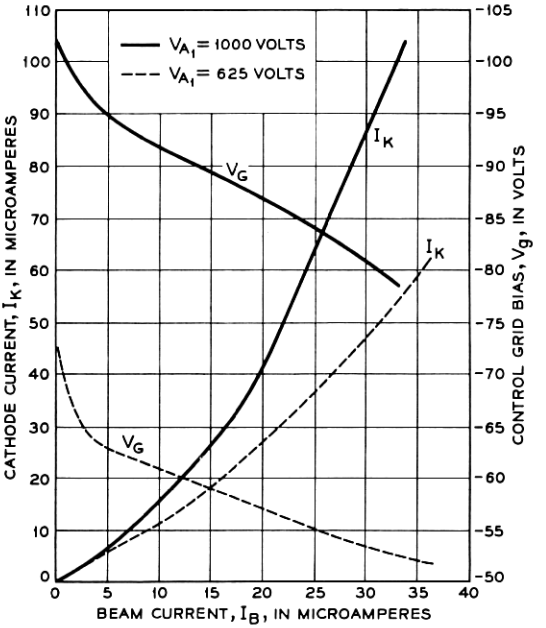

Fig. 16 — Tetrode gun characteristics.

V_{A_2} = 10 kilovolts. It is worth noting that the current efficiency I_B/I_K increases markedly as V_{A_1} is reduced from 1000 to 625 volts. This is due to the convergent lens action of the A_1–A_2 electrodes, as discussed in Section III.

7.1 σ_{avg} *as a Function of* V_{A_1} *and* V_{A_2}

One of the system objectives is to maintain the mean spot size, σ_{avg}, at a constant value of 0.0045 inch for all tubes. Because of the extreme sensitivity to gun electrode spacings, it is quite difficult to control spot size to that degree of precision from tube to tube when the crossover is formed by an immersion-lens gun. Therefore some electrical control of σ_{avg} is desirable, which can be done very conveniently in this CRT design by means of the first anode, A_1, potential. Fig. 17 is a plot of σ_{avg} vs V_{A_1} for a typical tube. It may be seen that a relatively wide σ_{avg} range, from 0.0040 to 0.0048 inch, is achieved as V_{A_1} is decreased from 1000 to 500 volts. The 0.0045 inch system objective is attained in a typical tube with V_{A_1} = 625 volts. Also shown in Fig. 17 is the change in optimum V_{A_3} and V_{A_4} focus voltages with V_{A_1}. A very desirable feature of the

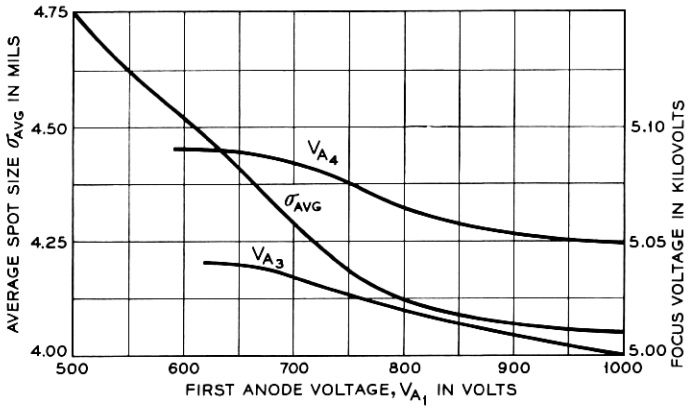

Fig. 17 — Focus voltages and σ_{avg} as a function of V_{A1}.

gun and lens design is that this variation is small, less than a one per cent increase (50 volts) in both V_{A_3} and V_{A_4}, as V_{A_1} is reduced from 1000 to 600 volts.

Another interesting capability of the CRT is that of decreasing σ_{avg} by changing the A_2 potential of the tetrode gun (the last aperture of the crossed-elliptical lens, and all subsequent electrodes are maintained at 10 kilovolts). The reason for this is that the magnification M is proportional to $\sqrt{V_{A_2}/V_{acc}}$. Fig. 18 is a plot of σ_{avg} as a function of V_{A_2} for $V_{A_1} = 1$ kilovolt, and the final accelerating potential, $V_{acc} = 10$ kilovolt.

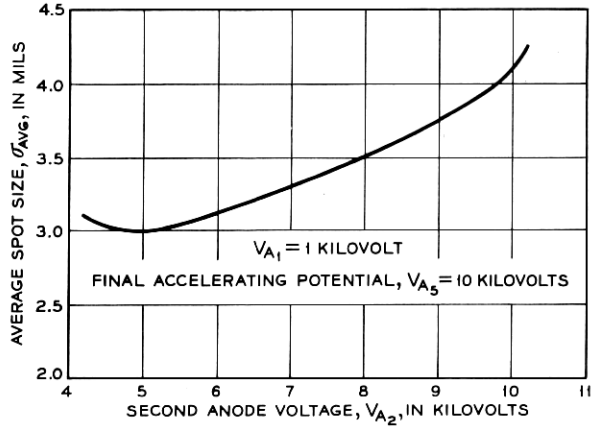

Fig. 18 — Average spot size as a function of V_{A_2}.

The average σ value may be reduced to as low as 0.003 inch by this technique, but it should be noted that current efficiency is decreased. Also, as may be seen from Fig. 23, the spot size uniformity ratio is inherently degraded with decreasing σ. This is because $\Delta D/\sigma$ increases at lower σ values, which results in an enlarged $\Delta\sigma/\sigma$ value. Since the system was designed for σ_{avg} at 0.0045 inch, V_{A_1}, rather than V_{A_2}, is varied to control the value of σ.

7.2 *Uniformity of Radiant Flux from Screen*

A typical distribution curve of radiant light flux from the quality screen area is given in Fig. 19. The brightest and dimmest spots are 20 per cent above and 30 per cent below the mean light output respectively. However, the radiant flux of over 95 per cent of the quality area is within a range of ± 10 per cent of the median output level. It should be pointed out that precision screen settling techniques are required to achieve the relatively narrow distribution of Fig. 19. Important considerations are rigid dust control in the settling room, removal of oversize phosphor particles, uniform screen weight, and aluminizing techniques which yield a smooth continuous aluminum layer. Also, it was found that the aging operation, in addition to removing the long decay time component of P16, produced a more uniform radiant flux distribution.

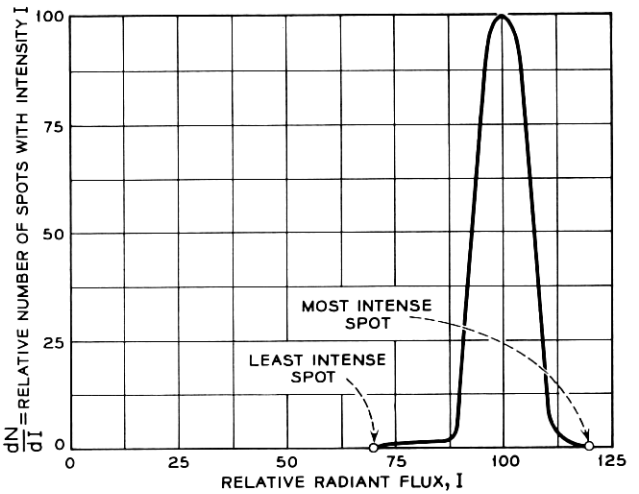

Fig. 19 — Typical distribution curve of light output from quality area.

VIII. SUMMARY AND CONCLUSIONS

Generalized step-by-step procedures have been presented for designing large-area electrostatically deflected cathode ray tubes for high and exceedingly uniform resolution. Both electron gun and electrostatic deflection plate design have been theoretically analyzed. Equations were evolved which yield an optimum combination of resolution, spot uniformity, and tube length.

There are three basic electron-optical design problems, namely those of the deflection system, electron gun, and lens. They may be summarized as follows:

1. Deflection plate length and deflection to screen distance are designed such that the maximum spot size enlargement, $\Delta\sigma_{max}$, produced by deflection distortion is the same for both pairs of plates and is exactly equal to the maximum permissible value. Equations for computing $\Delta\sigma_{max}$ as a function of beam size σ were derived for the case of deflection plates contoured for maximum sensitivity. Plate contour and minimum separation were then selected to provide the desired sensitivity, the separation between the plates in a given set being made as large as possible to reduce fringing field and deflection focusing aberrations. A novel feature that resulted from this work was a dual shield between the two pairs of plates which provides a substantial reduction of deflection aberrations.

2. A tetrode gun design is described which has properties of small crossover size, low cathode current density, high current efficiency, and low magnification M of the crossover at the screen. Equations for M have been developed, from which the minimum value of M can be found when the focal lengths and principal planes of the lens formed by the first and second anodes are known. Once the M value is fixed, the overall tube length is then determined from the deflection-to-screen distance obtained in step 1.

3. The electron lens and limiting aperture size are selected such that aberrations of both the lens and deflection fringing field are sufficiently small.

Using the above design principles, a cathode ray tube has been developed for the flying spot store which has exceptional spot size uniformity and meets system objectives. Typical performance characteristics of this tube are a Gaussian beam size, σ, of 0.0045 ± 0.0006 inch which can be maintained over a 6- by 6-inch square screen area for all beam currents from 4 to 20 microamperes without changing focus potentials. The 0.0045-inch σ value corresponds to a resolution of 2000 TV lines per useful target diameter and is electrically variable by controlling the first anode potential.

The faceplate is very flat (greater than 1900-inch radius), of moderate optical quality, and very free of flaws (less than 0.004-inch diameter with a minimum spacing of 0.050 inch). Precision preparation methods of the settled P16 screen yield a very uniform radiant (or light) flux output (typically within +20 and −30 per cent of the median value) at all points in the quality area.

IX. ACKNOWLEDGMENTS

Many people have made development of the flying spot store CRT possible. The project was under the general direction of J. A. McCarthy and R. W. Sears, whose suggestions and guidance have been most valuable. C. Maggs and J. W. West directed the faceplate development and mechanical design aspects of the work. Other important contributors are: G. E. Helmke and A. Pfahnl, development of the screen settling techniques; M. Poulsen, glass-to-metal faceplate seal; A. M. Johnson and J. J. Ulozas, tube evaluation and processing; and H. W. Ericsson and G. J. Kossyk, mechanical design.

APPENDIX A

The electron optical focusing action on the electron beam as it passes from the crossover to screen is depicted in Fig. 20(a). There are two lenses, the A_1–A_2 gap and the objective lens, which act to image the crossover onto the target. The purpose of this appendix is to compute the magnification M of the complete lens system. Fig. 20(b) shows the principal planes, object, image, and focal points of the two lenses. Conventional electron lens terminology[7] is used, where the quantities are positive as shown in Fig. 20(b). A beam acceleration from 1 to 10 kilovolts occurs at the A_1–A_2 gap, and it should be regarded as a thick rather than a thin lens.[7] Hence, it has two principal planes, P_1 for the object space and P_1' for the image space. Focal lengths are f_1 and f_1' respectively for object and image. Likewise, the distances from object and image points to their respective focal points are X_1 and X_1'. Similar notation holds for the objective lens, except that this lens is an einzel type and can to a good approximation be represented as a thin lens (Ref. 13, pp. 98–101). Thus the principal planes are coincident ($P_2 = P_2'$) and also $f_2 = f_2'$. It should be noted that Fig. 20(b) is drawn to indicate positive lens parameters and that actually the image point of the A_1–A_2 lens will lie beyond the target outside the tube, with the result that X_2 is negative. Also, the object focal point of the A_1–A_2 lens can be to the left of the crossover, and X_1 then becomes negative.

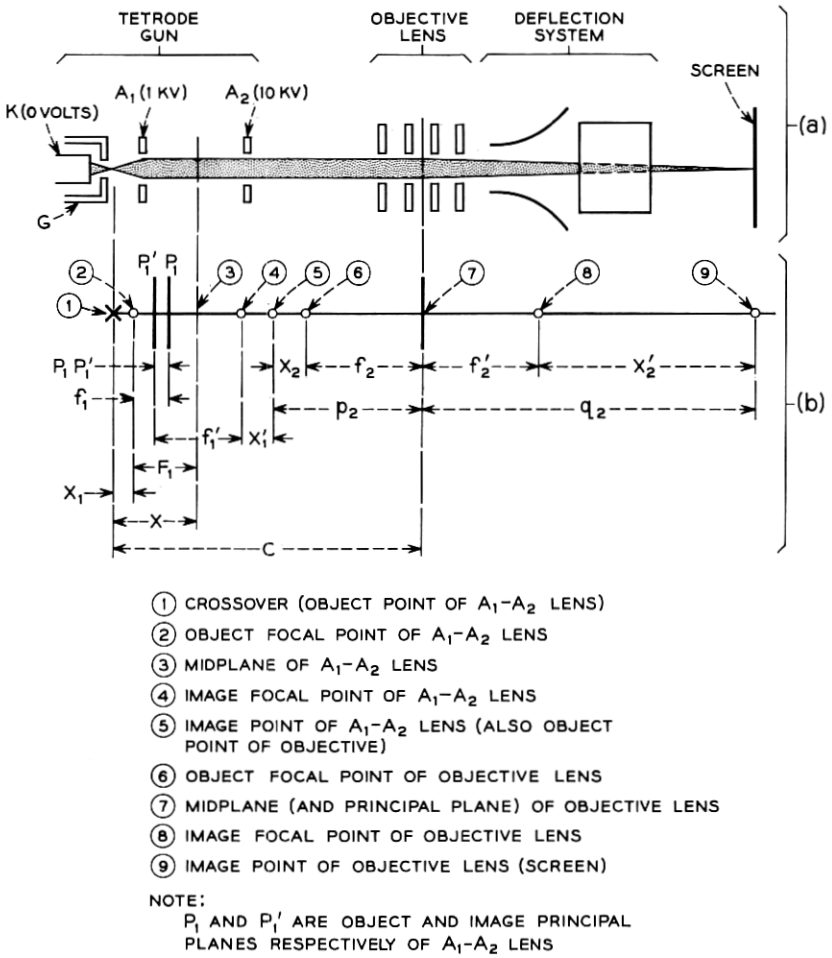

Fig. 20 — Notation used for calculation of crossover magnification M by A_1–A_2 and objective lenses.

First, the magnification M_1 of the A_1–A_2 lens and M_2 of the objective lens will be computed independently and then the combined magnification M of the two lenses in series will be derived. The thick-lens formula must be used for the A_1–A_2 lens, and the magnification M_1 is given by

$$M_1 = \frac{f_1}{X_1} = \frac{X_1'}{f_1'}, \tag{7}$$

where the quantities are as shown in Fig. 20(b). For the case of the thin lens (objective lens) $f_2 = f_2'$ and the expression for M_2 is therefore[7]

$$M_2 = \frac{X_2' + f_2}{X_2 + f_2} = \frac{q_2}{p_2}. \tag{8}$$

The total magnification M of both lenses[7] is

$$M = M_1 M_2 = \frac{f_1}{X_1} \frac{q_2}{p_2}. \tag{9}$$

Now the distance C in Fig. 20(b) between the crossover and objective lens midplane, a basic design value of the tube, is equal to

$$C = p_2 + X_1' + f_1' + X_1 + f_1 - \overline{P_1P_1'}. \tag{10}$$

Substituting (10) into (9), the expression for M becomes

$$M = \frac{f_1}{X_1} \frac{q_2}{(C + \overline{P_1P_1'} - X_1 - f_1 - X_1' - f_1')}. \tag{11}$$

The image distance X_1' and image focal length f_1' of the A_1–A_2 lens can be eliminated from (11) by the fundamental electron lens equations,[7]

$$X_1' = \frac{f_1 f_1'}{X_1}, \qquad f_1' = \sqrt{\frac{V_2}{V_1}} f_1. \tag{12}$$

Equation (11) then becomes

$$M = \frac{f_1 q_2}{X_1 \left(C + \overline{P_1P_1'} - X_1 - f_1 - \sqrt{\frac{V_2}{V_1}} \frac{f_1^2}{X_1} - \sqrt{\frac{V_2}{V_1}} f_1 \right)}. \tag{13}$$

Note that signs for all quantities in (13) must be carefully designated, where positive values are shown in Fig. 20. The distance X from the crossover to the midplane of the A_1–A_2 lens is given by relation

$$X = X_1 + F_1, \tag{14}$$

where F_1 is the focal length measured from the midplane.[7]

The parameters C and q_2 are basic design values of the tube and, for reasons of beam size, beam size uniformity, and deflection factor, were selected as $C = 5.0$ inches and $q_2 = 25.5$ inches. As mentioned previously $V_1 = 1$ kilovolt and $V_2 = 10$ kilovolts. Values of f_1, F_1, and $\overline{P_1P_1'}$ for electrode arrangements (a), (b), and (c) of Fig. 3 have been evaluated by Spangenberg and Field[8] and are tabulated in Table IV. Substituting these values in (13) and (14), the magnification M can then be

TABLE IV

A_1–A_2 Geometry (see Fig. 3)	f_1 (inches)	F_1 (inches)	$\overline{P_1P_1'}$ (inches)	$\frac{V_2}{V_1}$
(a) cylinder — aperture	0.8	1.3	0.15	10
(b) two cylinders of unequal diameter	1.2	3.2	−0.2	10
(c) two equidiameter cylinders	1.5	2.55	−0.9	10

computed as a function of the distance X from crossover to the A_1–A_2 midplane. The results are plotted in Fig. 4.

APPENDIX B

Spot size enlargement, $\Delta\sigma$, due to deflection focusing can be calculated from knowledge of the equivalent deflection plate focal length, f_D, and distance, p, from the center of deflection to the screen. It will be done in two steps. First the enlargement, ΔD, will be computed for a beam whose spot size is equal to zero at the undeflected screen position. Next the spot size increase, $\Delta\sigma$, for a Gaussian beam will be evaluated from ΔD.

It will be assumed that f_D can be represented by a thin convergent cylindrical lens with the principal plane at the center of deflection (the point at which the projected center of the deflected beam intersects the axis). The equivalent electron-optical diagram is shown in Fig. 9(c). If an ideal beam is focused by the objective lens, to a point o on the screen (σ = zero) at the undeflected position, and then deflection signals are applied, the distance q between the center of deflection and new focal point I (see Fig. 9) is

$$\frac{1}{-p} + \frac{1}{q} = \frac{1}{f_D} \qquad \text{or} \qquad q = \frac{pf_D}{p + f_D}. \tag{15}$$

The parameter p is the distance from center of deflection to screen and is the object point for the lens. It should be noted that, for convenience, p is defined positive for the object point to the right of the principal plane. Hence $-p$ must be used in the thin lens equation (15). The angle θ_B at which the beam converges to the image point I in Fig. 9(b) is

$$\theta_B = \frac{D_B}{q}. \tag{16}$$

where D_B is the beam diameter at the center of deflection. The enlargement ΔD is then, using (15) and (16),

$$\Delta D = (p - q)\theta_B = \frac{p}{f_D} D_B. \tag{17}$$

Spot size enlargement, $\Delta\sigma$, for a Gaussian beam can now be obtained from ΔD. It will be assumed for purposes of discussion, that the beam is deflected in the y direction, and attention will be confined only to the current density distribution $J(y)$ with its associated standard deviation σ_y. At the undeflected screen position, $J(y)$ is a Gaussian beam distribution denoted as $J_1(y)$ and is given by

$$J_1(y) = J_0 e^{-y^2/2\sigma_y^2}, \tag{18}$$

where J_0 is the current density at the beam center ($y = 0$). The integral of $J_1(y)\,dy$ from $-\infty$ to $+\infty$ is the beam current I_B, from which it may be shown that $J_0 = I_B/\sqrt{2\pi}\sigma_y$. Upon deflecting the beam to the maximum angle, $\theta_{\max}$, the Gaussian $J_1(y)$ appears in front of the screen at point 1 of Fig. 21. The value of σ_y probably will be reduced if the distance from 1 to the screen becomes large, but for high resolution CRT's this effect should be of second order and therefore will be neglected here. As illustrated in Fig. 21, a point y_1 on the Gaussian at position 1 becomes enlarged to an area ΔD at the screen. Thus there is a new (and enlarged) distribution $J_2(y)$ at the screen given by

$$J_2(y) = \int_{y-(\Delta D/2)}^{y+(\Delta D/2)} \frac{J_1(y_1)\,dy_1}{\Delta D}. \tag{19}$$

The distribution $J_2(y)$ is no longer a Gaussian but, if ΔD is sufficiently small, it will not deviate greatly. Hence, in order to retain the previous spot size definition of σ, it will be assumed that J_2 is also a Gaussian and can be written as

$$J_2(y) = J_0' e^{-y^2/2(\sigma_y+\Delta\sigma_y)^2},$$

where $J_0' = I_B/\sqrt{2\pi}(\sigma_y + \Delta\sigma_y)$ and $\Delta\sigma_y$ is the spot size enlargement.

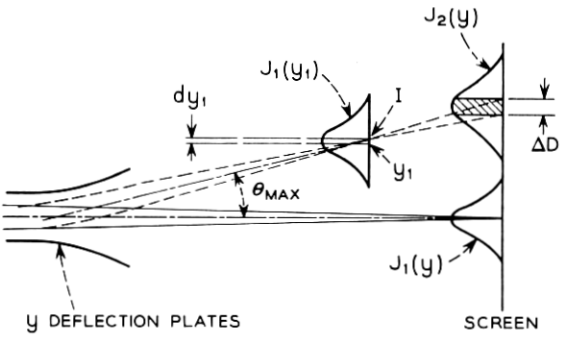

Fig. 21 — Relation of ΔD to Gaussian beam.

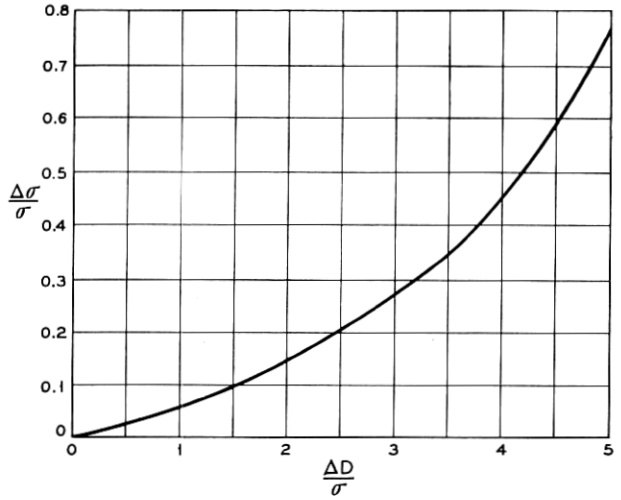

Fig. 22— Generalized relation of $\Delta\sigma$ to ΔD.

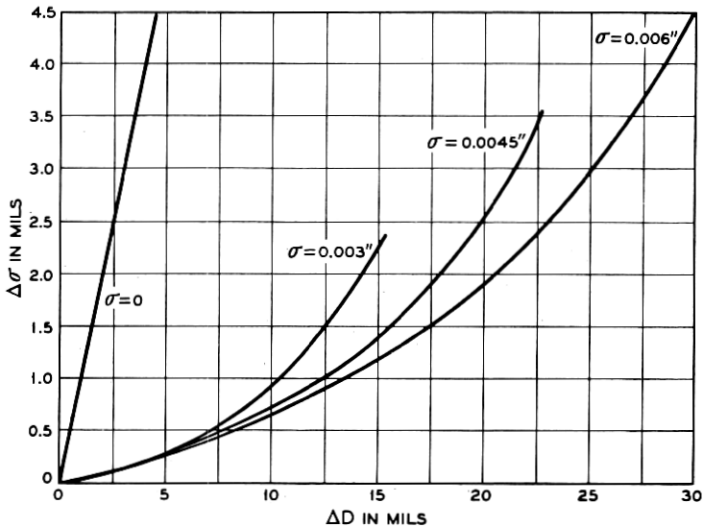

Fig. 23 — Enlargement $\Delta\sigma$ of a Gaussian beam as a function of zero beam size enlargement ΔD.

When $y = 0$, $J_2(y) = J_0'$ and (19) becomes

$$\frac{I_B}{\sqrt{2\pi}(\sigma_y + \Delta\sigma_y)} = \int_{-\Delta D/2}^{+\Delta D/2} J_0 \frac{e^{-y_1^2/2\sigma_y^2}}{\Delta D}\, dy_1. \tag{20}$$

By defining $u = \Delta D/2\sqrt{2}\sigma_y$, (20) may be solved for $\Delta\sigma_y/\sigma_y$, with the result

$$\frac{\Delta\sigma_y}{\sigma_y} = \frac{2u}{\sqrt{\pi}\ \text{erf}\ u} - 1, \tag{21}$$

where erf u is as defined in (5) of Section V. Equation (21) can be solved graphically and a plot of $\Delta\sigma/\sigma$ versus $\Delta D/\sigma$ is presented in Fig. 22 [the y subscripts in (21) are dropped in order to generalize]. In Fig. 23, $\Delta\sigma$ is shown as a function of ΔD for specific σ values of 0.003, 0.0045, and 0.006 inch. It may be noted that $\Delta\sigma$ increases superlinearly with ΔD. Also it decreases markedly with increasing σ at a fixed ΔD value. Thus it becomes clear that, when one is designing a CRT for a high degree of spot size uniformity (low $\Delta\sigma$), improvements are obtained at an exponential rate as ΔD is reduced and/or σ_{avg} is increased.

REFERENCES

1. Hoover, C. W., Jr., Staehler, R. E., and Ketchledge, R. W., Fundamental Concepts in the Design of the Flying Spot Store, B.S.T.J., **37,** 1958, p. 1161.
2. Hoover, C. W., Jr., Haugk, G., and Herriott, D. R., System Design of the Flying Spot Store, B.S.T.J., **38,** 1959, p. 365.
3. Joel, A. E., Jr., An Experimental Switching System Using New Electronic Techniques, B.S.T.J., **37,** 1958, p. 1091.
4. Cooper, H. G., McCarthy, J. A., and Sears, R. W., A High-Resolution CRT Employing Electrostatic Deflection, I.R.E. Prof. Group on Electron Devices Meeting, Washington, D. C., October 30, 1959.
5. Klemperer, O., *Electron Optics*, 2nd ed., Cambridge Univ. Press, Cambridge, 1953, p. 254.
6. Moss, H., The Electron Gun of the Cathode Ray Tube, J. Brit. I.R.E., **5,** 1945, p. 10; **6,** 1946, p. 99.
7. Spangenberg, K. R., *Vacuum Tubes*, McGraw-Hill, New York, 1948, Ch. 13.
8. Spangenberg, K. R., and Field, L. M., The Measured Characteristics of Some Electrostatic Electron Lenses, Elect. Comm., **21,** 1943, p. 194.
9. Spangenberg, K. R., and Field, L. M., Some Simplified Methods of Determining the Optical Characteristics of Electron Lenses, Proc. I.R.E., **30,** 1942, p. 138.
10. Kirkpatrick, W. E., et al., to be published.
11. Greenwood, T. S., and Staehler, R. E., A High-Speed Barrier Grid Store, B.S.T. J., **37,** 1958, p. 1195.
12. Maloff, I. G., and Epstein, D. W., *Electron Optics*, McGraw-Hill, New York, 1938, p. 200.
13. Pierce, J. R., *Theory and Design of Electron Beams*, 2nd ed., D. Van Nostrand, New York, 1954.
14. Peirce, B. O., *A Short Table of Integrals*, 3rd ed., Ginn & Co., Boston, p. 116.